Forest Ecology and Management 572 (2024) 122305

Contents lists available at ScienceDirect

Forest Ecology and Management

journal homepage: www.elsevier.com/locate/foreco

Characterizing the competitive stress of individual trees using point clouds

Ghasem Ronoud [a,*], Maryam Poorazimy [a], Tuomas Yrttimaa [a], Antero Kukko [b], Juha Hyyppä [b], Ninni Saarinen [a], Ville Kankare [c], Mikko Vastaranta [a]

[a] School of Forest Sciences, University of Eastern Finland, Joensuu 80101, Finland
[b] Department of Remote Sensing and Photogrammetry, Finnish Geospatial Research Institute, National Land Survey of Finland, Espoo 02150, Finland
[c] University of Turku, Department of Geography and Geology, Turku FI-20014, Finland

ARTICLE INFO

Keywords:
Airborne laser scanning (ALS)
Boreal forest
Competition indices
Growth
Terrestrial laser scanning (TLS)
Silviculture

ABSTRACT

The competitive stress of individual trees can be quantified by considering their positions and dimensions such as diameter at breast height (dbh) and height with respect to their neighbor trees. However, measurements of these attributes in the field limit the number of trees and stands that can be assessed with given resources. In recent years, terrestrial laser scanning (TLS) and airborne laser scanning (ALS) data have become prominent in characterizing three-dimensional forest structures. These data could also provide efficient and reliable tools to assess the competitive stress of trees within a stand. Therefore, we aimed to investigate the capability of TLS and low-altitude ALS in characterizing the competitive stress affecting individual trees in boreal forests. We compared: a) an object-based approach that quantified competition through the identification and characterization of competing neighbor trees from the TLS and ALS point clouds, and b) a point cloud-based approach where the presence of point cloud structures representing competitive vegetation around a target tree was considered. Accordingly, three object-based competition indices (CIs) utilizing dbh (CI_{dbh}), height (CI_H), and maximum crown diameter (CI_{MCD}) as weights were calculated using the Hegyi equation. For the point cloud-based approach, the canopy density index (CDI), and the competitive pressure index (CPI) were derived using an upside-down search cone set at 60 % relative tree height, while the $CI_{Cylinder}$ was calculated by counting the number of voxels occupied by the competitive vegetation inside a fixed-radius cylinder. These laser scanning-based CIs were assessed against *in situ*-based CIs where dbh and height were used as weights in the Hegyi equation. The results showed that the object-based CIs were more correlated ($r = 0.33$–0.48, p-value < 0.001) with the *in situ*-based CIs in comparison with the point cloud-based CIs ($r = -0.22$–0.37). The object-based CIs showed a high correlation ($r = 0.65$–0.71, p-value < 0.001) when compared between TLS and ALS, while a greater variation was observed for the point cloud-based CIs ($r = 0.29$–0.53, p-value < 0.001). Tree detection rate and the number of neighboring trees in the field affected how well the CIs derived from the TLS and ALS data were in line with the *in situ*-based CIs, especially when the competitive stress was assessed using the object-based CIs. In conclusion, the object-based CIs derived using TLS and ALS provided consistent characterization of competition in managed boreal forests compared to the *in situ*-based CIs. While TLS is ideal for small-scale assessments, low-altitude ALS offers a rather similar capacity for assessing competition but with broader coverage. In complex forest structures, reliable tree detection is essential to avoid underestimating the competitive stress of trees.

1. Introduction

Forests are dynamic and complex ecosystems, and their growth depends on a variety of biotic and abiotic factors such as macro- and microclimate conditions, soil fertility, water availability, plant functional traits, human-induced harvest, forest management, and competitive interaction between individual trees (Burkhart and Tomé, 2012; Fichtner and Härdtle, 2021; Stephenson et al., 2014). Competition between individuals is a crucial factor, affecting how individual trees can utilize the available growth resources and thus affecting how they

* Corresponding author.
E-mail addresses: ghasem.ronoud@uef.fi (G. Ronoud), maryam.poorazimy@uef.fi (M. Poorazimy), tuomas.yrttimaa@uef.fi (T. Yrttimaa), antero.kukko@nls.fi (A. Kukko), juha.hyyppa@nls.fi (J. Hyyppä), ninni.saarinen@uef.fi (N. Saarinen), viveka@utu.fi (V. Kankare), mikko.vastaranta@uef.fi (M. Vastaranta).

https://doi.org/10.1016/j.foreco.2024.122305
Received 11 June 2024; Received in revised form 16 September 2024; Accepted 17 September 2024
Available online 25 September 2024

grow (Hui et al., 2018; Perry, 1985). Trees that outcompete others can benefit more from resources such as growing space, water, sunlight, and soil nutrients (Tomé and Burkhart, 1989). Hence, monitoring competition between individuals can provide ecological insights for forest managers and stakeholders (Pedersen et al., 2013). The magnitude of competition is also an effective input parameter for a variety of models describing forest development such as basal area growth (Bollandsås and Næsset, 2009), recruitment (Lexerød and Eid, 2005), and mortality (Eid and Tuhus, 2001). Therefore, competition must be quantified to understand its effects on tree growth and forest ecosystem dynamics (Pitkänen et al., 2022; Twery and Weiskittel, 2013).

Competition between trees is typically quantified using competition indices (CIs) such as the Hegyi index, which are based on the size and location of a target tree relative to its neighboring trees (Burkhart and Tomé, 2012). A target tree refers to an individual tree within a forest stand that competes with its neighboring trees for resources and is influenced by the negative impact of neighboring trees. The use of CIs to describe the competition between trees has proven to be robust but often requires *in situ* data which can be labor-intensive and time-consuming to acquire. In addition, the number of feasible tree attributes to be used for computing CIs is rather limited (Burkhart and Tomé, 2012; Tompalski et al., 2016; Wensel et al., 1987). Especially for characterizing tree crown expansion, accurately measuring the crown size in the field using conventional mensuration tools is practically impossible (Ma et al., 2018; Weiskittel et al., 2011). The crown size, instead, can be estimated by using allometric models based on dbh and height, but it is prone to uncertainty (Wensel et al., 1987). In addition, measuring crown structure by *in situ* measurements needs destructive sampling. Therefore, it is necessary to develop alternative approaches to assess competition between trees to improve understanding of tree and forest growth processes (Ma et al., 2018; Olivier et al., 2016).

Laser scanning offers methods to collect three-dimensional (3D) information on forests at a wide range of scales (Bazezew et al., 2018; Giannetti et al., 2018; Su et al., 2016; Tempel et al., 2015; Wulder and Franklin, 2003). Laser scanning characterizes trees and forests by emitting laser pulses from a sensor, which bounce off surfaces like tree crowns and stems, with the returning signals used to create point cloud enabling 3D reconstruction of the forest structure. Terrestrial laser scanning (TLS) is a close-range sensing technique that, besides the stem dimensions, can obtain detailed information about tree crown structures (Maas et al., 2008; Muhojoki et al., 2024; Rocha et al., 2023). TLS is most effective when collecting information on individual trees, sample plots, or a limited number of stands. TLS data is acquired through static measurements from a tripod. From a single scanning location, it is only possible to measure such trees that are directly visible to the scanner. Still, it can provide detailed information about the measured trees, including the dimensions of the stem and branches (Raumonen et al., 2013). When collecting data from a sample plot or a stand, TLS measurements from multiple scanning locations are used. This allows for a more complete reconstruction of the trees to be characterized, though the process is labor-intensive and thus costly (Liang et al., 2016; White et al., 2016). On the other hand, airborne laser scanning (ALS) is a powerful technique that can capture tree and forest structures on a large scale (Axelsson et al., 2023; Maltamo et al., 2006; Su et al., 2016). One ALS survey can cover hundreds of thousands of hectares, making it suitable for gathering data supporting forest planning and operations. ALS data are collected from above the canopy and thus it is best suited for measuring canopy height and tree density. In contrast to TLS measurements, ALS does not (yet) provide detailed information on tree stems due to considerably lower point density (Casas et al., 2016; Hyyppä et al., 2012; Poorazimy et al., 2022; Su et al., 2016; Vauhkonen et al., 2014). Considering the above capabilities, TLS and ALS present new opportunities also for describing the competition among trees. Previous studies have shown the potential of point cloud-based assessment of competition between trees by identifying and characterizing the target trees and their neighboring trees considered as competitors (Lin et al., 2016; Pont et al., 2021; Ronoud et al., 2022). This approach is called the object-based approach as the identification and characterization of competitors occurs at the object level (i.e., the individual tree level). Like *in situ*-based CIs, the size and location of neighboring trees relative to the target tree are used for computing CIs (Ma et al., 2018). On the other hand, laser scanning point clouds can be directly used to estimate competition between trees (Metz et al., 2013; Olivier et al., 2016; Pedersen et al., 2013, 2012; Seidel et al., 2015; Yrttimaa et al., 2022). In this approach, hereafter referred to as the point cloud-based approach, the competitive stress is characterized based on the co-existence of vegetative structures around the target tree (Metz et al., 2013). For instance, Olivier et al. (2016) used TLS point clouds to investigate the response of sugar maple (*Acer saccharum* Marshall) crowns to competition and highlighted the capability of point cloud-based CIs in describing space occupancy. In a recent study, Yrttimaa et al. (2022) investigated the effect of interactions between individual trees and their neighbors on stem growth, suggesting the potential of point cloud-based CIs. Nevertheless, the characterization of competition using point clouds is still in the early stage and remains a topic that necessitates further investigation and understanding (Lo and Lin, 2013; Ma et al., 2018; Metz et al., 2013; Pedersen et al., 2012; Yrttimaa et al., 2022).

Laser scanning technologies are widely used to collect forest resource information in many countries to collect forest resource information, supporting especially silviculture, forest planning, and timber procurement (Fassnacht et al., 2024). Additionally, various laser scanning techniques are being increasingly employed to support forest science research (Calders et al., 2020). Detecting and describing the competition between trees is one thematic area where laser scanning is expected to provide solutions, both in research and practical forestry. For this reason, understanding how competition can be described using ALS and TLS data, and how well these descriptions align with each other and with traditional approaches with *in-situ* measurements, will help forest researchers identify the best ways to describe competition. It will also assist end-users in understanding the strengths and weaknesses of competition described through point clouds, enabling them to make informed decisions.

Therefore, this study aimed to provide insights into the capability of TLS and low-altitude ALS in characterizing competitive stress affecting individual trees. Specifically, we addressed three research questions: (1) How well do object-based and point cloud-based CIs characterize competition between trees when compared to competition as characterized using *in situ* data? (2) Are competition assessments derived using TLS and ALS data consistent? and (3) how does the number of neighboring trees in the field around the target tree and the tree detection rate affect the estimation errors of CIs assessed using laser scanning?

2. Materials and methods

2.1. Site description and in situ data

This study was carried out in the Evo study site (61°19.6′ N, 25° 10.8′ E), located in the southern boreal forest of Finland (Fig. 1). The study site covers approximately 2000 ha of mainly Scots pine (*Pinus sylvestris*, L.), and Norway spruce (*Picea abies* (L.) H. Karst.) dominated forests with elevation in the study area ranging from 125 m to 182 m above sea level.

The experimental design of this study consists of 22 rectangular sample plots with a size of 32 m × 32 m (Fig. 1) that were established in 2014 to support the TLS benchmarking project that aimed to investigate various TLS approaches for forest inventory and assess the effect of forest structure on the accuracy and completeness of tree attribute extraction using TLS data (Liang et al., 2018). The sample plots were selected to represent a range of stand conditions typical of boreal forests, considering factors such as development stage, stem density, sub-canopy vegetation density, and species composition (Liang et al., 2018). Therefore, the selected plots encompass a variety of forest structures,

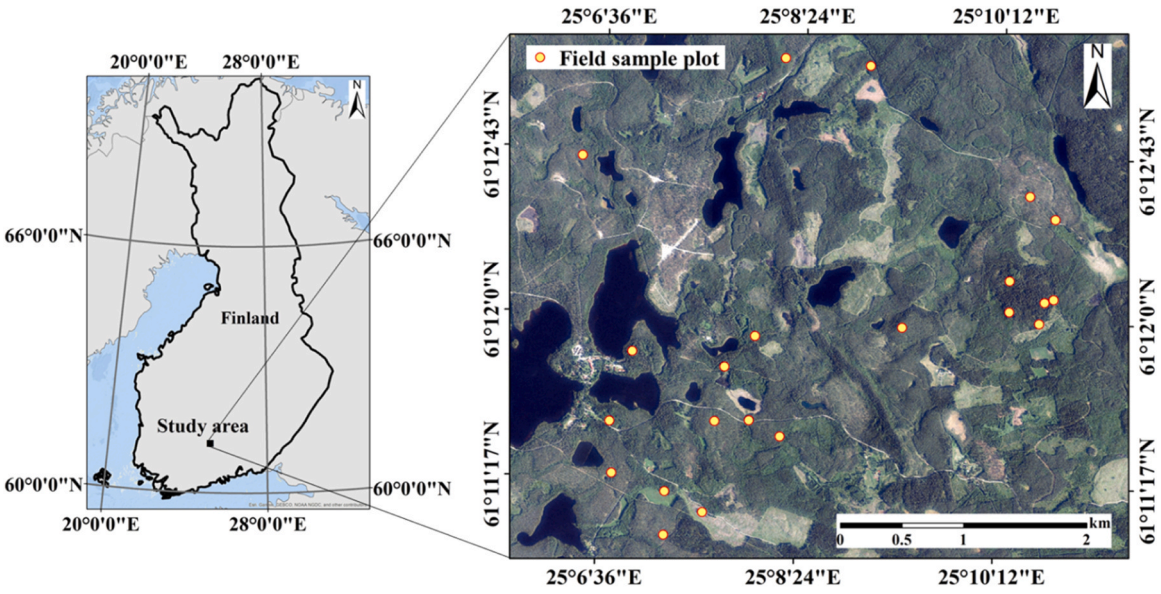

Fig. 1. A map showing the location of the study area in Evo, Finland, and the distribution of the sample plots on top of aerial imagery.

comprising both managed and single-layered, as well as unmanaged and multi-layered forests (Fig. 2). *In situ* measurements in the field were carried out during the summer of 2014. The location of each sample plot was defined by utilizing the geographic coordinates of the plot center and its four corners. Plot center coordinates were recorded using a Trimble 5602 DR200 + total station which was oriented to the local coordinate system using ground control points. The Trimble R8 Global Navigation Satellite System (GNSS) receiver (Trimble lnc., CA, USA) was implemented to measure ground control points in open areas, close to the plot.

In each sample plot, all trees with a dbh greater than 5 cm were measured and recorded. The dbh of trees was measured with calipers as an average of two measurements from two directions perpendicular to each other. Tree height was measured with an electronic clinometer. During the measurements, tree species were recorded for each tree.

Table 1
Summary statistics of the structural characteristics of the sample plot based on *in situ* measurements including the Minimum (Min), Mean, Maximum (Max), and Standard deviation (std.) of the number of trees per hectare (N), mean volume (V), mean diameter weighted by basal area (D_g), and mean height weighted by basal area (H_g).

Attribute	N (n/ha)	V (m^3/ha)	D_g (cm)	H_g (m)
Min	430	110.64	13.91	13.03
Mean	1238	297.24	25.93	21.01
Max	3008	482.33	41.58	27.04
Std.	731	115.21	9.10	4.14

Fig. 2. Illustration of the spectrum of boreal forest stand conditions investigated in this study: managed and single-layered (left) and unmanaged and multi-layered (right) structures.

Table 1 summarizes the structural characteristics of the sample plots based on the *in situ* measurements.

2.2. Laser scanning data acquisition

2.2.1. Low altitude airborne laser scanning (ALS)

In December 2014, the acquisition of ALS point clouds was conducted using a Riegl VQ-480-U scanner (RIEGL Laser Measurement Systems GmbH, Austria) from a helicopter flying at an altitude of 75 m to acquire high-density point clouds. The Riegl VQ-480-U scanner provides a field of view of 60° and operates at a laser beam wavelength of 1550 nm featuring a beam divergence of 0.3 mrad. During the data acquisition, the scan speed was set to 150 Hz and pulse repetition rate to 550 kHz. The flight speed was kept constant at 50 km/h. The ground footprint size, on-ground pulse spacing along the scan line, and on-ground pulse spacing between scan lines were approximately 2.3 cm, 4.7 cm, and 9.3 cm, respectively. To ensure data quality, manual removal of error points was performed. Points originating from erroneous returns, such as isolated points in the sky or below the ground level, were carefully identified and eliminated from the dataset. The resulting ALS point clouds exhibited a point density of approximately 450 points/m^2, indicating high detail and precision in the captured information (Table 2).

2.2.2. Terrestrial laser scanning (TLS)

The TLS point cloud data acquisition was conducted during the spring of 2014 using a Leica HDS6100 (Leica Geosystems, St. Gallen, Switzerland) phase-shift scanner. The scanner operated at a wavelength of 690 nm and was capable of capturing high-density point clouds with a scanning rate of 508,000 points per second. The resulting point cloud from a single scan exhibited a hemispherical (310° vertical × 360° horizontal) coverage, providing detailed information in both the vertical and horizontal directions, with an angular resolution of 0.018° (Table 2). A multi-scan approach was employed to acquire comprehensive point clouds for each sample plot. This approach involved conducting five individual scans from distinct locations. The scan configuration consisted of a center scan positioned at the plot's center, supplemented by four auxiliary scans strategically placed at the quadrant directions (i.e., northeast, southeast, southwest, and northwest), approximately 11 m away from the plot center. A co-registration process was performed to integrate the individual scans and generate a unified point cloud. This process involved aligning the scans using artificial reference targets as control points. The Z + F LaserControl point cloud processing software was utilized in this co-registration procedure. Following successfully merging the scans, the resulting point clouds were utilized to locate trees within each sample plot. Tree maps were subsequently created by manually identifying the cross-sections of individual trees from horizontal slices of the TLS point clouds. The tree maps were verified in the field and augmented with missing trees (mostly small in diameter) not identified from the point cloud slices.

2.3. Detecting and characterizing trees using TLS and ALS

The TLS and ALS were classified into ground and non-ground points using LAStools software. Using the lidR package, triangulated irregular network (TIN) models were created to generate TLS and ALS-based digital terrain models (DTMs) with a resolution of 0.5 m (Roussel and Auty, 2018). Then, the TLS and ALS point clouds were normalized using the respective DTMs, and only points representing vegetation were chosen for further analysis.

The TLS and ALS-derived canopy height models (CHMs) were generated from the height-normalized TLS and ALS point clouds using the pit-free algorithm (Khosravipour et al., 2016) in the LAStools software. The pit-free algorithm operates by utilizing respectively a standard CHM and partial surface models generated from all and the highest return points close to pits. In this study, to obtain partial CHMs, a set of 2, 5, 10, 15, 20, 25, 30, 35, and 40 m height thresholds were considered. For this task, the normalized point clouds were thinned with half of the pixel size. To fill potential holes, a near-ground surface model was also generated by excluding points above 10 cm (Isenburg, 2019). Finally, the generated CHM and partial surface models were aggregated as one, final CHM with a pixel size of 0.5 m based on the highest values selected from all the CHM or partial surface models.

To perform the analysis at the level of individual trees, a local maxima filter (LMF) algorithm with an experimentally checked fixed window size of 3 × 3 pixels, was implemented to the final CHM of a sample plot to find the treetops using the lidR package of R. Then, using a marker-controlled watershed segmentation algorithm (Meyer and Beucher, 1990) the final CHM was segmented into individual tree crowns (i.e., 2D crown segments). Obtained tree crown segments were used to clip out the points belonging to each tree using a point-in-polygon approach applied to the XY plane.

The classification of TLS-derived individual tree point clouds was conducted using the methodology initially developed by Yrttimaa et al. (2020). It is based on the separation of points originating from a stem and crown. It was completed by applying surface normal filtering and random sample consensus (RANSAC)-cylinder filtering procedures to finally identify point cloud clusters forming smooth, vertical, and cylindrical structures considered to represent a tree stem. An alpha shape was created to envelop these points, while points remaining outside the alpha shape were assumed to represent the tree crown. ALS point clouds delineated by individual trees were classified as crown points if they existed outside the alpha-shape and within the 2D crown segment. Finally, individual tree locations from the TLS point clouds were determined by calculating the center points of RANSAC cylinders fitted into the stem points at the breast height (i.e., XY coordinates), and for ALS, the mean XY coordinates of all points within each 2D crown segment were used.

Tree height was determined based on the highest point return within each tree segment. Moreover, to derive the crown structure and relevant geometric features, a 2D convex hull object was employed to enclose the

Table 2
Summary of terrestrial laser scanning (TLS) and airborne laser scanning (ALS) acquisition characteristics.

Characteristic	TLS	Helicopter-borne ALS
Scanner	Leica HDS6100	Riegl VQ−480-U
Wavelength	690 nm	1550 nm
Beam divergence	0.22 mrad	0.3 mrad
Field of view	310° vertical × 360° horizontal	60°
Date	Spring, 2014	Winter, 2014
Platform	Tripod	Low-altitude helicopter

Table 3
Stem and crown attributes derived from terrestrial laser scanning (TLS) and/or airborne laser scanning (ALS) point clouds. dbh_{TLS}: diameter at breast height (dbh) derived from TLS point clouds; dbh_{ALS}: the dbh predicted based on ALS-derived tree height; H_{TLS}: The tree height derived from TLS point clouds; H_{ALS}: The tree height derived from ALS point clouds; MCD_{TLS}: Maximum crown diameter derived from TLS point clouds; MCD_{ALS}: Maximum crown diameter derived from ALS point clouds; $CA_{2D\text{-}TLS}$: the Crown area derived from TLS point clouds; $CA_{2D\text{-}ALS}$: the Crown area derived from ALS point clouds.

Attribute (unit)	Description/ Calculation
dbh_{TLS} /dbh_{ALS} (cm)	The diameter at breast height (1.30 m) of the individual trees obtained by fitting a RANSAC cylinder/dbh was predicted using allometry (Kalliovirta and Tokola, 2005) with tree height.
H_{TLS} and H_{ALS} (m)	The maximum height (Z value) of individual tree point clouds for TLS and ALS.
MCD_{TLS} and MCD_{ALS} (m)	Maximum crown diameter based on the 2D convex hull for TLS and ALS.
$CA_{2D\text{-}TLS}$ and $CA_{2D\text{-}ALS}$ (m^2)	Area of the crown 2D convex hull projected onto XY plane for TLS and ALS.

crown points of TLS and ALS using the rLiDAR package. This enabled the characterization of the crown morphology based on the two key crown attributes, namely 2D crown area (CA_{2D}) and maximum crown diameter (MCD) (Table 3). Table 3 shows the computed attributes characterizing individual trees using the TLS and ALS point clouds.

The dbh of individual trees was either directly measured (TLS) or predicted based on tree height (ALS). With TLS, the dbh was derived by fitting RANSAC cylinders into stem points delineated from multiple heights around the breast height (i.e., at height intervals of 1.25–1.30 m and 1.30–1.35 m). Finally, the mean of these consecutive diameter observations at the different heights around the breast height was considered as the dbh estimate (Table 3). For those trees that the dbh measurement was not logical (i.e., did not fall between ~5 cm to ~65 cm) or could not be obtained at all, then the dbh was predicted based on tree height using allometric models (Kalliovirta and Tokola, 2005). This was done due to the limited capacity of characterizing all the trees by TLS acquisition in this study. For example, some trees had not fully been scanned from all directions, leading to an incomplete point cloud characterization which tends to lead to overestimating dbh based on the point cloud-based diameter measurements. With ALS, the dbh was predicted using the same equation based on tree height (Kalliovirta and Tokola, 2005).

2.4. Quantifying competitive stress of individual trees using TLS and ALS

2.4.1. Object-based approach

In the object-based approach, competitive stress for each target tree within the plot was quantified based on the size and locations of their neighboring trees. We used a fixed 8 m distance around each target tree as a search radius for determining neighboring trees affecting competition, as suggested by previous studies (Pedersen et al., 2012; Pont et al., 2021; Zhou et al., 2022). Three spatially explicit CIs were calculated for each target tree as a sum of inverse distances to the neighboring trees weighted by the i) dbh (CI_{dbh}), ii) tree height (CI_H), and iii) tree maximum crown diameter (CI_{MCD}) according to the Hegyi equation (Hegyi, 1974) (Eq. 1).

$$CI = \sum_{i=1}^{n} (X_i/(X \times dist_i)) \quad (1)$$

where the competition index for a given individual target tree is denoted as CI, n represents the total number of neighboring trees located within the search radius; X_i represents the dbh, height, and maximum crown diameter (MCD) of the i^{th} neighboring tree, X refers to the corresponding dbh, height, and MCD of the target tree, and $dist_i$ denotes the horizontal distance (m) between the target tree and the i^{th} neighboring tree. To account for the effect of topography on CIs based on tree height, non-normalized height was restored via DTMs. It is worth mentioning that the computation of CIs for trees located closer than 8 m distance from the plot border was excluded to avoid edge effects. This also allowed us to ensure that the TLS scan setup provides a complete, multi-viewpoint reconstruction of the trees (Yrttimaa et al., 2019).

2.4.2. Point cloud-based approach

In the point cloud-based approach, the competitive stress affecting target trees was computed using two different approaches for finding the vegetative structures of neighboring trees causing competition: 1) a search-cone method which includes canopy density index (CDI) and competitive pressure index (CPI), and 2) a search cylinder method. Because of the topography effect on the estimated CIs, the non-normalized TLS and ALS point clouds were used in our study (Yrttimaa et al., 2022). Of importance, the CIs were not computed for the trees closer than 8 m distance from the plot border to avoid the edge effect as applied in the object-based approach.

The CDI and CPI were determined based on canopy occupancy within the crown neighborhood and the geometric relationship between the target tree and its neighbors. To this end, according to Seidel et al. (2015), an upside-down cone with an opening angle of 60° and a vertical orientation was positioned at a height corresponding to 60 % relative tree height (Fig. 3). By enveloping a horizontal cross-section of non-stem points of each target tree with a 2D convex hull, we determined the small-end diameter of the search cone at that height. Using the non-normalized point clouds of the sample plots, we delineated points that fell inside the search cone but remained outside the 3D convex hull of the target tree crown and considered them as the neighboring points. In the next step, these neighboring points were voxelized to a 0.1 m × 0.1 m × 0.1 m grid. Therefore, each point in this voxelized neighboring point cloud represented 0.001 m^3 of vegetation-occupied space around the target tree's crown. The CDI and CPI were computed using the neighboring point clouds, the search cone's geometry, and the target tree's crown characteristics. The first step involved volumetric analysis of the occurrence of vegetative structures within the competitive space. We considered the volume of the space occupied by the neighboring point clouds (CV) as the number of neighboring points (with Z ≤ height of the target tree) multiplied by their representative volume of 0.001 m^3. The CDI (i.e., the relative volume of the space occupied by neighboring trees) was calculated as the ratio between the CV and the volume of the search cone whose top surface was constrained to the height corresponding to the tree height (V_{cone}) excluding the volume of the target tree's crown (V_{crown}). The geometric equation of a truncated cone volume was used to compute the V_{cone}. To consider the distance of the neighboring trees, a 3D version of the CPI (2D version of CPI proposed by Olivier et al. (2016) was implemented. Here, the CPI was calculated as a mean inverse Euclidean distance between the neighboring points and the surface of the 3D convex hull of the target tree

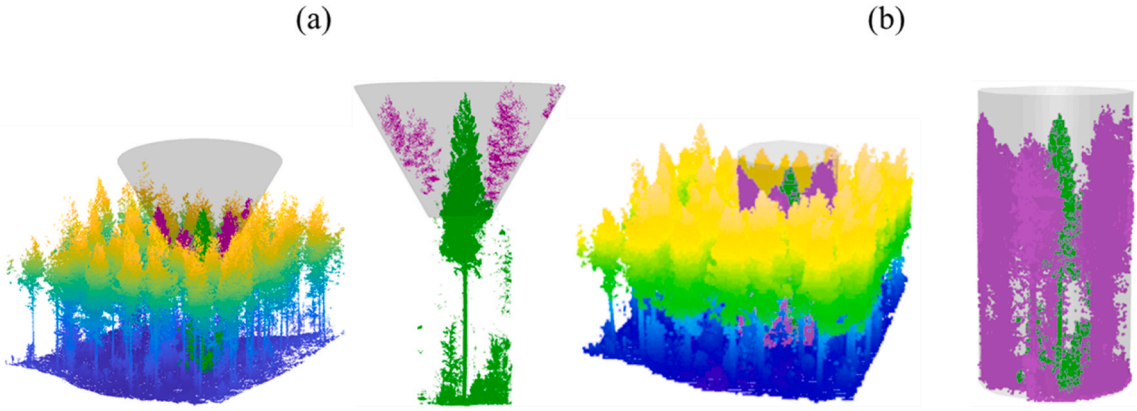

Fig. 3. Illustration of (a) the Search-cone method and (b) the Cylinder-based method to describe the competition between trees. The target tree is shown as green, while point cloud structures considered to represent the competing neighbors are shown in purple.

crown (Fig. 3).

In the search cylinder method, determining the filling of cylindrical space was notably simpler compared to conical filling due to the absence of the necessity for conversion into spherical coordinates (Seidel et al., 2015). Therefore, the number of 1 dm^3 voxels with centers located within a 4 m radius search cylinder were counted and the respective vegetation-occupied volume was determined, $CI_{Cylinder}$ (Fig. 3). Following Seidel et al. (2015), we used the 4 m radius search cylinder due to its better performance compared to smaller or larger-sized search cylinders according to our initial experiments. This choice was influenced by the findings that smaller cylinders failed to encompass an adequate amount of vegetative to effectively replicate competitive stress affecting target trees, while larger cylinders potentially included vegetative structures no longer relevant for contributing to the competitive stress (Seidel et al., 2015).

2.5. Quantifying competitive stress of individual trees using in situ data

The reliability of the CIs derived from laser scanning techniques and different approaches was assessed based on competition indices derived from *in situ* data. The Hegyi equation using dbh ($CI_{dbh\text{-}In\ situ}$) and height ($CI_{H\text{-}In\ situ}$) was implemented in the same way as the object-based CIs to compute the magnitude of competition affecting each *in situ* target tree (Sections 2–4–1). The edge effect was also considered by excluding the computed *in situ*-based CIs for trees closer than 8 m distance from the plot border. It is worth mentioning that $CI_{H\text{-}In\ situ}$ was only used to assess the accuracy of estimated CI_H, while other CIs were assessed against $CI_{dbh\text{-}In\ situ}$. Based on findings obtained in previous studies, relative basal area increment has also been used to assess the reliability of CIs (Contreras et al., 2011; Hui et al., 2018; Pedersen et al., 2013; Rivas et al., 2005; Seidel et al., 2015; Szwagrzyk et al., 2012) and thus it was also included as an *in situ* CI in this study. The basal area increment was calculated by subtracting the *in situ* basal area in 2014 from the respective measure in 2021 and dividing the result by the initial basal area in 2014.

2.6. Tree-to-tree matching

Tree-to-tree matching was needed to assess the accuracy of CIs derived from TLS and ALS relative to their corresponding *in situ*-based CIs. This involved finding the corresponding field-measured tree for each tree derived from the TLS point clouds (i.e., TLS trees) and the ALS point clouds (ALS trees). The matching process aimed to minimize both geospatial error and tree height error between the point cloud-derived and *in situ* measured tree attributes. For this purpose, the similarity in the geospatial locations of TLS and ALS trees with the *in situ* trees within a maximum 2 m distance was considered. In case multiple detected or *in situ* trees were located within the applied search distance, the correspondences were determined based on similarity in their tree height. This matching procedure and applied constraints resulted in a total number of 225 TLS and 213 ALS trees to be analyzed (Table 4). Due to the systematic acquisitions of point clouds, it is assumed that these trees are representative of trees that can be characterized by laser scanning point clouds in varying boreal forest conditions. For the matched trees, the correlation between dbh derived from TLS and *in situ* measurements was 0.77, and for height, it was 0.94. Similarly, the correlation between dbh derived from ALS and *in situ* measurements was 0.68, while for height, it was 0.96. Table 4 summarizes their structural attributes and CIs. The TLS and ALS trees were also matched using the above-mentioned tree-to-tree matching methodology to assess the consistency of TLS- and ALS-derived CIs, resulting in 126 trees being included in both datasets.

Table 4
Minimum (Min), Mean, Maximum (Max), and Standard deviation (Std.) of structural attributes and competition indices (CIs) for the matched trees of terrestrial laser scanning (TLS) and airborne laser scanning (ALS) as well as their *in situ* correspondence. The dbh, H, and MCD indicate tree diameter at breast height, height, and maximum crown diameter. CI_{dbh}, CI_H, and CI_{MCD} are the object-based CIs based on dbh, H, and MCD respectively. The canopy density index (CDI), competitive pressure index (CPI), and $CI_{Cylinder}$ (i.e. vegetation-occupied volume) are point cloud-based CIs. From the TLS point clouds, 225 trees could be identified and matched with the *in situ* trees, while the corresponding number for the ALS point clouds was 213. This accounts for the small differences in the characteristics of the *in situ* trees between the TLS and ALS datasets.

Attribute / Competition index (CI)	Dataset	Min	Mean	Max	Std
dbh (cm)	*In situ*	5.25	20.03	38.80	7.17
	TLS	8.25	21.61	36.24	5.95
	In situ	5.25	20.32	38.80	6.76
	ALS	13.32	24.27	35.04	4.97
H (m)	*In situ*	10.40	20.50	30.20	4.62
	TLS	12.57	20.95	29.45	3.94
	In situ	10.50	20.92	30.20	4.38
	ALS	11.58	21.03	30.32	4.29
MCD (m)	TLS	2.92	5.21	7.72	6.89
	ALS	2.31	5.21	8.53	1.21
CI_{dbh}	*In situ*	0.63	1.84	7.95	1.06
	TLS	0.95	2.41	4.60	0.77
	In situ	0.63	1.70	2.93	0.51
	ALS	0.63	1.95	3.56	0.73
CI_H	*In situ*	0.83	1.82	2.77	0.45
	TLS	1.27	2.39	3.56	0.55
	In situ	0.83	1.82	2.77	0.45
	ALS	0.52	1.93	3.47	0.71
CI_{MCD}	TLS	0.74	2.37	4.16	0.77
	ALS	0.34	2	4.03	0.74
CDI	TLS	0.0005	0.03	0.08	0.02
	ALS	0	0.006	0.015	0.004
CPI	TLS	0.5	89.51	242.82	57.68
	ALS	0	16.10	54.58	11.99
$CI_{Cylinder}$	TLS	6322	64949	124297	27151.59
	ALS	0	4935	11352	2872

2.7. Assessment of the capability of point clouds in characterizing competitive stress in trees

The relationships between the laser scanning-derived object-based and the point cloud-based CIs and the *in situ*-based CIs were assessed using Pearson's correlation coefficient (r). It is important to note that $CI_{H\text{-}In\ situ}$ was used solely to evaluate the accuracy of the estimated CI_H, while the other CIs were evaluated against $CI_{dbh\text{-}In\ situ}$. Based on the correlation analysis, it was also assessed which of the *in situ*-based CIs, the CI_{dbh}/CI_H or the basal area increment, had a stronger association with the laser scanning-based CIs. A high value for r implies a strong relationship between the ALS/TLS-based and *in situ*-based CIs, which would indicate the feasibility of using point clouds to assess the competitive stress of individual trees. Notably, the TLS-based CIs were assessed with $n = 225$, while the ALS-based CIs were assessed with $n = 213$.

Consistency between the TLS-based CIs and respective ALS-based CIs was assessed for the 162 trees that were included in both datasets using r as a measure of the level of consistency. A high value for r implying a strong relationship between the ALS-based and the TLS-based CIs would indicate that the measures derived from terrestrial point cloud data are consistent with the measures derived from aerial point cloud data.

To better understand the performance of the applied methodologies in boreal forest conditions, we further analyzed possible differences between the TLS/ALS-based and *in situ*-based CIs and investigated the effects of forest structural variability in the observed differences (ΔCIs). As the object-based CIs – both laser scanning-based and *in situ*-based – were computed using the Hegyi equation, the respective CI values were

directly comparable while the point cloud-based CIs were represented by different scales than the *in situ*-based CIs (see Table 4). Thus, for the object-based CIs the respective ΔCIs were computed by subtracting the *in situ*-based CI_{dbh} values from the laser scanning-based CI values. For the point cloud-based CIs, the original CI values were first rescaled by dividing with the maximum observed values. The ΔCIs were then computed by subtracting the rescaled *in situ*-based CI_{dbh} values from the laser scanning-based CI values.

Based on current knowledge, it is known that the capacity of laser scanning to detect trees decreases as the density of a forest stand increases (Maltamo et al., 2004; Yrttimaa et al., 2019). Considering the definition of the spatially explicit CIs based on the Hegyi equation, an incomplete tree detection within the competitive neighborhood of a target tree (i.e., within an 8-m distance) would lead to an erroneous CI estimate. All this considered, it can be assumed that the more trees there are surrounding and competing with the target tree, the more uncertainty can be expected for the laser scanning-based CI estimates. To find this out, we first assessed the relationship between ΔCIs and the number of competitor trees as identified based on the *in situ* measurements using *r* as the measure of the strength of the relationship. In addition, we also investigated the association between the plot-level tree detection rate and the density of trees within the sample plot to better understand the effect of forest structure on the capacity of laser scanning point clouds to characterize the competitive stress of trees, where the detection of trees is of importance for accurate CI estimation. It is worth mentioning that the above-mentioned relationships were also assessed for statistical significance using *p*-values.

3. Results

3.1. The relationship of object-based and point cloud-based CIs with the in situ-based CIs

The results of correlation analysis between the laser scanning-derived object-based and the point cloud-based CIs and the *in situ*-based CIs are presented in Table 5. In most cases, the CIs based on the *in situ* data were more correlated with the laser scanning-based CIs than the *in situ* relative basal area increment (Table 5). The CDI_{TLS} was the only index that was more correlated with the *in situ* relative basal area increment ($r = 0.25$ and p-value < 0.001). The capacity of the laser scanning point clouds to capture the competitive status of trees varied depending on the applied CI with correlations up to 0.44 and 0.48 recorded with TLS and ALS, respectively (Table 5). The strongest relationship was recorded between the CI_{dbh} of TLS and the $CI_{dbh\text{-}in\ situ}$ CI ($r = 0.48$ with p-value < 0.01). Generally, the object-based CIs derived from laser scanning were more correlated with the *in situ*-based CI ($r =$ 0.33–0.48) than the point cloud-based CIs ($r = -0.22$–0.37). The $CI_{Cylinder}$ of TLS ($r = 0.37$) and ALS ($r = 0.23$) was the highest correlated point cloud-based CIs with the $CI_{dbh\text{-}in\ situ}$. While the CDI_{TLS} showed a weak correlation with the *in situ*-based CI ($r = 0.18$ with p-value < 0.01), there was no correlation found between the CDI_{ALS} and $CI_{dbh\text{-}in\ situ}$ ($r = -0.03$, p-value > 0.05). The CPI_{ALS} was negatively associated with the $CI_{dbh\text{-}in\ situ}$ with $r = -0.22$ (p-value < 0.05).

3.2. The consistency of object- and point cloud–based CIs derived from TLS and ALS data

Fig. 4 shows the correlation between the TLS CIs and the respective ALS CIs as a measure of consistency. The object-based CIs had a higher correlation between TLS and ALS ($r = 0.65$–0.71, p-value < 0.001) than the point cloud-based CIs ($r = 0.29$–0.53, p-value < 0.001). Among the object-based CIs, the CI_H showed the highest correlation of 0.71 between TLS and ALS. In terms of point cloud-based CIs, the CDI had the highest correlation between TLS and ALS ($r = 0.53$), followed by $CI_{Cylinder}$ ($r = 0.45$, p-value < 0.001) and the CPI ($r = 0.29$, p-value < 0.001).

3.3. The effect of forest structure on the TLS and ALS CIs

The effects of forest structure on the capacity of TLS and ALS point clouds for describing the competition between individual trees are depicted in Figs. 5 and 6. The difference between the laser scanning-based CIs and the *in situ*-based CIs (ΔCIs) increased as the number of neighboring trees around the target in the field tree increased, especially for the object-based CIs ($r = -0.79$ to -0.96, p-value < 0.001) (Fig. 5). This was also observed for the CDI, with both TLS ($r = -0.42$, p-value < 0.001) and ALS ($r = -0.57$, p-value < 0.001), as well as for the TLS ($r = -0.56$, p-value < 0.001) and ALS-based ($r = -0.72$, p-value < 0.001) CPI (Fig. 5). Among all object and point cloud-based CIs, the $CI_{Cylinder}$ showed the lowest correlation with the number of neighboring trees around the target in the field, with a correlation of -0.32 for TLS (p-value < 0.001) and -0.33 for ALS (p-value < 0.001) (Fig. 5).

Respectively, the ΔCIs decreased and approached zero as the plot-level tree detection rate increased (Fig. 6). In general, the object-based CIs were more affected by the detection rate ($r = 0.68$–0.84, p-value < 0.001) compared to point cloud-based CIs ($r = 0.25$–0.49, p-value < 0.001). The $CI_{Cylinder}$ showed the lowest correlation with the plot-level tree detection rate, with a correlation of 0.25 for TLS (p-value < 0.001) and 0.28 for ALS (p-value < 0.001) (Fig. 6). The relationship between plot-level detection rate of TLS and ALS data and plot-level *in situ* tree density has been provided in Fig. 7. As shown, both TLS and ALS plot-level tree detection rates were highly correlated with plot-level tree density in the field ($r = \geq 0.8$, p-value < 0.001).

Table 5
Pearson's correlation coefficients (*r*) and *p*-value measuring the statistical significance of the relationship between the competition indices (CIs) derived from terrestrial (TLS) and airborne laser scanning (ALS) and the *in situ* data. CI_{dbh}, CI_H, and CI_{MCD} are object-based CIs based on tree diameter at breast height, height, and maximum crown diameter, respectively. The canopy density index (CDI), competitive pressure index (CPI), and $CI_{Cylinder}$ (i.e. vegetation-occupied volume) are point cloud-based CIs. The *in situ*-based CIs include the $CI_{dbh\text{-}In\ situ}$ for assessing all ALS and TLS-derived CIs except CI_H, which was assessed using $CI_{H\text{-}In\ situ}$. The statistical significance denoted as ns (not significant): p-value > 0.05, *: p-value < 0.05, **: p-value < 0.01, and ***: p-value < 0.001.

Type of competition index	Competition index (CI)	Dataset	*In situ*-based CI		*In situ* relative basal area increment	
			Correlation (*r*)	*p*_value	Correlation (*r*)	*p*_value
Object-based	CI_{dbh}	TLS	0.48	$4.47\times10^{-14***}$	−0.09	0.22^{ns}
		ALS	0.44	$1.58\times10^{-11***}$	0.13	0.07^{ns}
	CI_H	TLS	0.40	$3.95\times10^{-10***}$	−0.14	0.037^{*}
		ALS	0.43	$6.7\times10^{-11***}$	0.13	0.06^{ns}
	CI_{MCD}	TLS	0.33	$4.33\times10^{-7***}$	−0.15	0.02^{*}
		ALS	0.44	$1.72\times10^{-11***}$	0.09	0.22^{ns}
Point cloud-based	CDI	TLS	0.18	$8.5\times10^{-3**}$	0.25	$2.09\times10^{-4***}$
		ALS	−0.03	0.72^{ns}	0.04	0.55^{ns}
	CPI	TLS	0.03	0.65^{ns}	0.03	0.67^{ns}
		ALS	−0.22	$1.41\times10^{-3**}$	−0.18	$9.46\times10^{-3**}$
	$CI_{Cylinder}$	TLS	0.37	$1.72\times10^{-8***}$	−0.18	$9.37\times10^{-3**}$
		ALS	0.23	$9.94\times10^{-4**}$	−0.06	0.4^{ns}

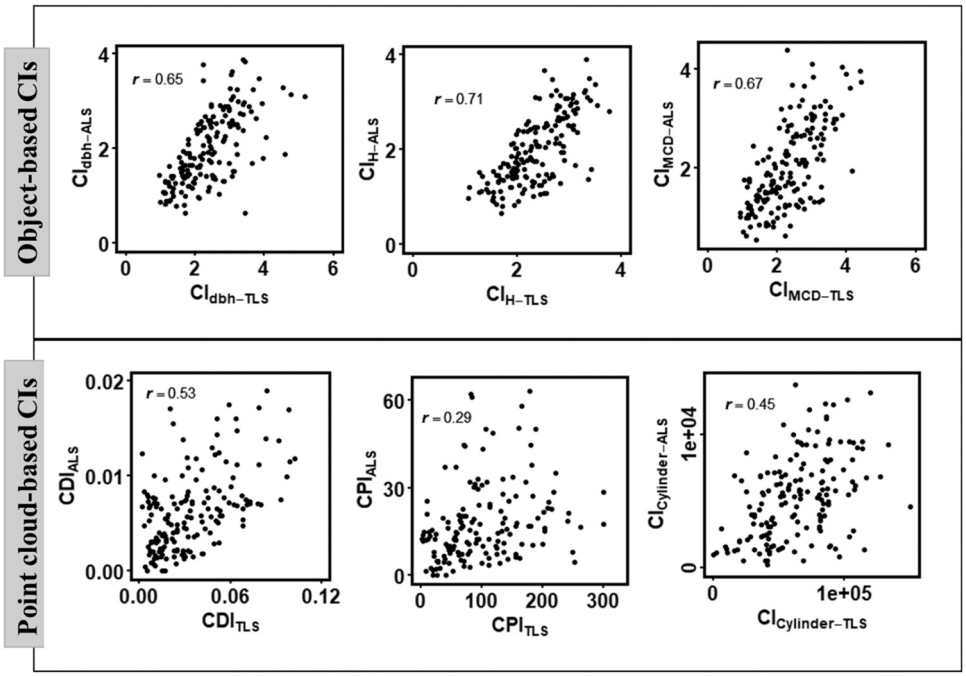

Fig. 4. Scatterplots and Pearson's correlation coefficients (*r*) show the consistency between competition indices (CIs) derived from terrestrial laser scanning (TLS) and airborne laser scanning (ALS). The investigated CIs were based on diameter at breast height (CI_{dbh}), height (CI_H), maximum crown diameter (CI_{MCD}) as well as canopy density index (CDI), competitive pressure index (CPI), and $CI_{Cylinder}$ (i.e. vegetation-occupied volume). All relationships were statistically significant with *p*-value < 0.001.

4. Discussion

This study aimed to investigate the capability of alternative laser scanning approaches for characterizing competitive stress affecting individual trees in boreal forests. Specifically, we characterized competition among individual trees using the point clouds directly (Point clouds-based CIs) and compared them to the more common object-based CIs. Our results showed that the object-based CIs derived from the TLS and low-altitude ALS point clouds had a higher correlation with the *in situ*-based CIs than the point cloud-based CIs. Additionally, we found that the CIs derived from the TLS and low-altitude ALS point clouds, particularly the object-based CIS, were correlated with each other. We observed, however, that the forest structure, particularly the number of neighboring trees and how well the trees were detected, affected how well the competition could be described. When the number of trees that were not detected from the point clouds was high, the competitive effects were underestimated. This impact was especially noticeable with the object-based CIs.

Some studies have found the current *in situ* relative basal area increment to be well correlated with competition (Pedersen et al., 2013; Seidel et al., 2015). Based on this study, the *in situ* relative basal area increment from 2014 to 2021 was less correlated with the TLS and ALS CIs than the *in situ*-based CIs computed by the Hegyi equation. Therefore, we compared the CIs (i.e. the competitive stress affecting the target trees in our study) derived from the TLS and ALS point clouds with the *in situ*-based CIs.

These point cloud-based CIs had lower correlations with the *in situ* CIs, which can be attributed to their different approach in characterizing competition compared to the *in situ* CIs. The object-based CIs were computed using the Hegyi equation, similar to the *in situ*-based CIs, with the only difference being the input data (i.e. tree attributes derived from TLS and ALS point clouds) used for the computations. The point cloud-based CIs aimed at quantifying the competitive stress through the magnitude of competitive vegetative structures occupying the assumed growing space of the target tree, which was assumed to better characterize the competition. Unlike the point cloud-based CIs, the shape of the crowns of the neighboring trees and how much they contributed to shading was not considered by the object-based CIs nor the *in situ*-based CIs, which could at least partly explain the differences in the correlations recorded between the point cloud-based and the *in situ*-based CIs. The simplified way of the Hegyi equation characterizing competition (i.e. considering the sum of inverse distances to all of its neighboring trees, weighted by their size) originates from the times when conventional *in situ* measurements were available. Based on our results, it appears that while describing competition using point cloud-based methods seems more appealing as point clouds characterize open and closed-space rather directly, competition effects described using object-based methods still align better with *in-situ* competition indicators. This raises the question of whether *in-situ* measurements represent the actual competition as well as possible, but we were unable to investigate this with our research setup and it remains to be explored in the future.

The CI_{dbh} provided the highest correlations with the *in situ*-based CIs, especially for TLS (Table 5). This difference could be attributed to the higher capability of TLS point clouds in characterizing tree stems rather than tree height or crown structure, especially in complex stands (Calders et al., 2020). However, tree height was also appropriate for describing competition using TLS and ALS point clouds because the CIs based on this attribute were significantly correlated with the corresponding $CI_{H\text{-}In\ situ}$ (Table 5). In a study conducted by Versace et al. (2019), CI_{dbh} and CI_H showed comparable levels of correlation with *in situ*-based competition, with R^2 values of 0.66 and 0.68, respectively. Contrary to our study, they estimated competition using ALS attributes by modeling with ordinary least square regression. Generally, the capability of ALS in characterizing the upper parts of tree crowns, especially in dense stands, is more effective than TLS due to their different point cloud acquisition geometries (Novotny et al., 2021). Hence, ALS performed slightly better than TLS to describe competition based on MCD (Table 5).

In terms of the point cloud-based CIs, the $CI_{Cylinder}$ exhibited a greater correlation with the $CI_{dbh\text{-}in\ situ}$ than the search-cone CIs (i.e. CDI and CPI) (Table 5). This was likely due to the contribution of the entire architecture of the neighboring trees to the competitive stress affecting

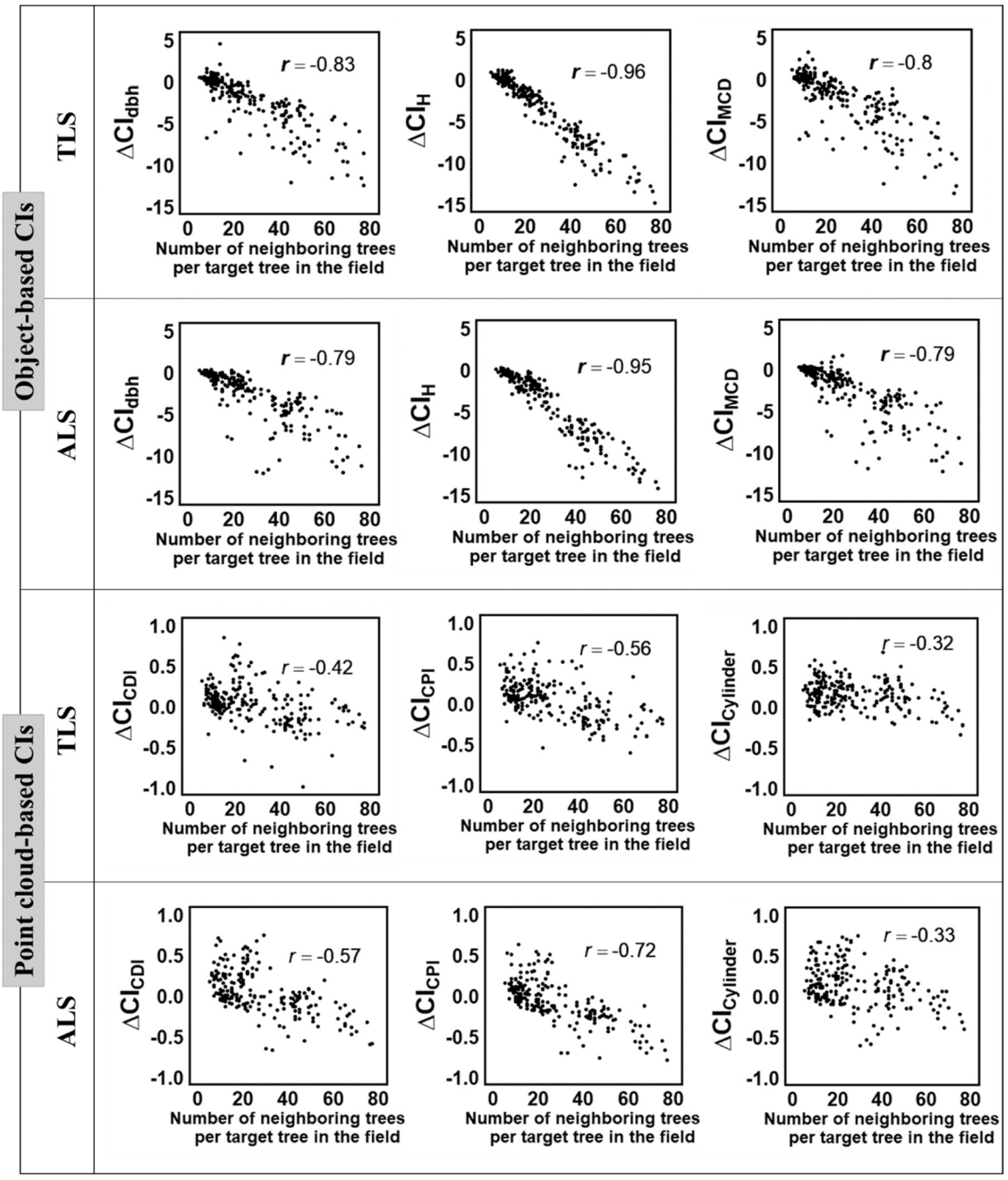

Fig. 5. Scatterplots and Pearson's correlation coefficients (*r*) illustrate the effect of the number of neighboring trees per target tree in the field on the difference (Δ) of competition indices (CIs) derived from terrestrial laser scanning (TLS) and airborne laser scanning (ALS) compared to the *in situ* data. The investigated CIs were based on diameter at breast height (CI_{dbh}), height (CI_H), maximum crown diameter (CI_{MCD}) as well as canopy density index (CDI), competitive pressure index (CPI), and $CI_{Cylinder}$ (i.e. vegetation-occupied volume). All relationships were statistically significant with *p*-value < 0.001.

the target trees that the $CI_{Cylinder}$ was able to characterize instead of the upper canopy structures considered by the CDI and CPI. Seidel et al. (2015) obtained similar conclusions when comparing cylinder and search cone methods to describe competition against *in situ* relative basal area increment. In the search cone methods, the CDI described competition between trees more effectively with TLS than with ALS, whereas the CPI did not show a similar relationship with the in-situ CIs (Table 5). In contrast, Olivier et al. (2016) found that the CDI derived from TLS point clouds was less important in explaining crown attributes compared to the CPI.

TLS and ALS observe the forest differently because of the distinct viewing angles and acquisition geometry (Hilker et al., 2012, 2010; Kükenbrink et al., 2017). In other words, TLS provides a different point cloud reconstruction of the trees compared to respective low-altitude ALS acquisition. Therefore, it could be worthwhile to expect that point cloud-based CIs differ depending on the point cloud type used. For instance, inconsistency between the CPI_{TLS} and the CPI_{ALS} can be attributed to the different occlusion effects due to measurement geometries (Fig. 4). With TLS, most of the occlusion occurs at the top and middle parts of the tree crown (Béland et al., 2014, 2011), while ALS provides a less-occluded view towards tree tops while being prone to neglecting lower canopy layers through dense canopies (Kükenbrink et al., 2017). The $CI_{Cylinder\text{-}TLS}$ was more correlated with the magnitude of the competition explained by *in situ* data than $CI_{Cylinder\text{-}ALS}$. This is

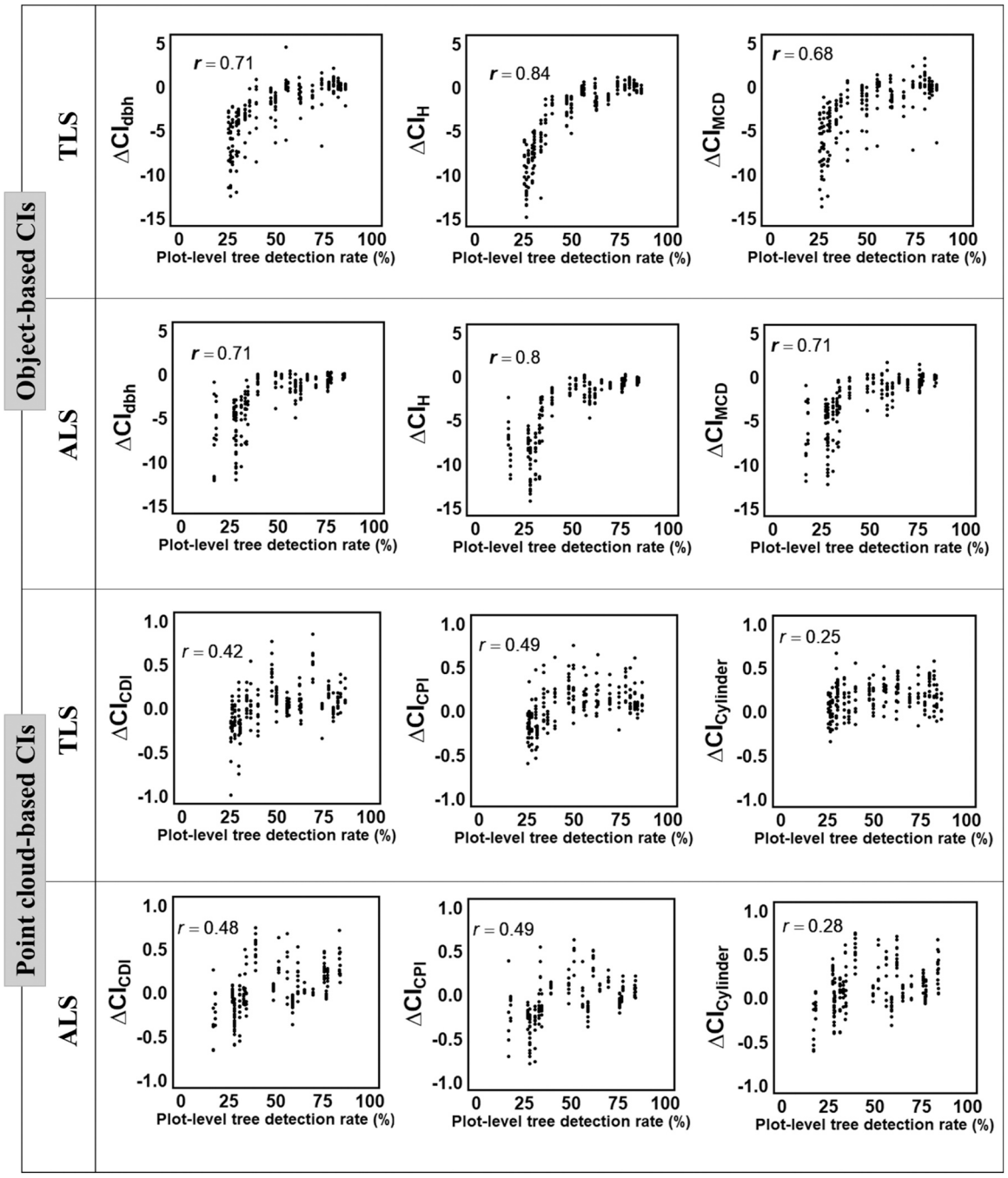

Fig. 6. Scatterplots and Pearson's correlation coefficients (r) illustrate the effect of plot-level tree detection rate on the difference (Δ) of competition indices (CIs) derived from terrestrial laser scanning (TLS) and airborne laser scanning (ALS) compared to the *in situ* data. The investigated CIs were based on diameter at breast height (CI_{dbh}), height (CI_H), maximum crown diameter (CI_{MCD}) as well as canopy density index (CDI), competitive pressure index (CPI), and $CI_{Cylinder}$ (i.e. vegetation-occupied volume). All relationships were statistically significant with p-value < 0.001.

likely caused due to the above-canopy viewpoint of ALS which cannot provide as detailed information on the horizontal structure of individual trees as TLS (Terryn et al., 2022). In other words, more voxels originated from tree stems in the TLS point clouds than in ALS point clouds due to the top-down viewing geometry, fewer observation angles, and smaller scan angle range of ALS (Kükenbrink et al., 2017). This comparison between the point cloud-based CIs of TLS and ALS revealed that TLS could generate a wider range of CI values compared to ALS (Fig. 4). This is likely due to the better capacity of TLS to capture the details of individual tree structures, especially in the lower parts of the crown and stem. This aspect became evident in the point cloud-based CIs associated with the number of voxels occupied by competitive vegetation. An adequate scan number and precisely determined scan positions can minimize crown occlusion in TLS acquisitions (Hilker et al., 2010). On the other hand, the object-based CIs derived using TLS and ALS were more closely associated with each other than point cloud-based CIs (Fig. 4). This rather high consistency resulted from the object-based nature of these indices to quantify competition.

In our study, both TLS and ALS underestimated the competitive status of trees compared to the *in situ* CIs, mainly due to their incapability of detecting all the competitive neighbor trees surrounding the target trees (Fig. 6). While our experimental setup included a limited

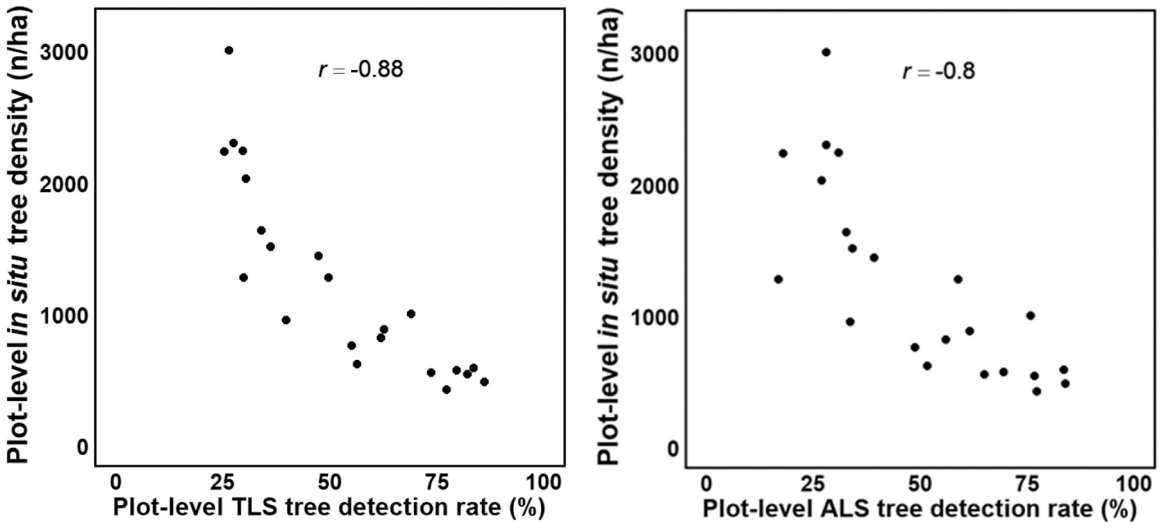

Fig. 7. Scatterplots of plot-level terrestrial laser scanning (TLS) and airborne laser scanning (ALS) tree detection rate vs. plot-level *in situ* tree density. All relationships were statistically significant with p-value < 0.001.

number of sample plots and trees to be investigated, the sampling was initially planned to feature a multitude of boreal forest structures. This enabled us to evaluate the assessment of laser scanning-based CIs within varying competitive conditions. We found out that in complex stands with multilayered canopies, mixed tree species, and dense understory, large trees are reliably identified, whereas small trees remain underrepresented (Maltamo et al., 2004; Yrttimaa et al., 2019). Under such circumstances, the precision of detecting trees using laser scanning is likely to be limited (Maltamo et al., 2004; Persson et al., 2002; Wang et al., 2016). The negative effect of forest structure as a primary factor on the accurate detection rate has been reported by Vauhkonen et al. (2012) when they compared six different methods across five sites of boreal forests for individual tree detection using ALS point clouds. Wang et al. (2016) also concluded that the lower detection rate arises from the complex forest structure due to the omission of intermediate and suppressed trees. They stated that the probability of correctly detecting intermediate and suppressed trees depends on the canopy morphology of neighboring trees as well as height variance (Wang et al., 2016). Neither of the applied laser scanning techniques (i.e. TLS and ALS) was able to detect all the trees (Fig. 7), which resulted in an underestimation of the affected competitive stress (Fig. 6).

Considering the definition of the applied CIs, it was crucial to identify all the neighboring trees when object-based CIs were used, as these CIs were computed as the sum of inverse distances to all neighboring trees within a search radius (here 8 m), weighted by their sizes in dbh, height, and MCD. And, neglecting even some of the trees considered as competing neighbors resulted in an underestimation of the competitive stress affecting the target tree. It is important to note that it is difficult to associate the estimation error of point cloud-based CIs such as CPI and $CI_{Cylinder}$ with the tree detection rate. This is because the detection rate does not necessarily reflect how well the surroundings of each target tree were characterized.

The novelty of this work lies in the comparison of point cloud-based and object-based CIs derived from TLS and low-altitude ALS for characterizing competition between individual trees. Specifically for object-based methods, we found that forest structure, especially the number of neighboring trees and the success of tree detection, influenced how well competition was described. Trees were not as well detected in dense forests, and when trees were not detected, the competitive effects were underestimated. This impact was particularly evident with the object-based approach. Importantly, the research underscores the limitations of the laser scanning-based approaches in complex forest environments where the dense and multi-story vegetation generates point cloud occlusion, resulting in the non-detection of competing neighbors surrounding the target trees. This challenge can be mitigated by careful planning of the data acquisition campaign where efforts should be put in acquiring complete point cloud reconstruction of all the tree individuals and to capture the full extent of vegetative structures within the competitive neighborhood of the target trees. It should be noted that the applied low-altitude ALS data acquired using a helicopter is still considered rather experimental and thus the related findings should be interpreted cautiously. However, it is anticipated that such data will become more operationally available in the future along with the development of sensor technology and the carrying capacity of alternative platforms such as unmanned aerial vehicles. Considering the complementary viewpoints of TLS and ALS, the fusion of terrestrial and aerial point clouds has been shown to benefit the characterization of individual trees (Dai et al., 2019) and it might provide a solution for CI estimation accuracy enhancement as well. Of importance, the automatic segmentation of point clouds is also prone to omission and inaccurate delineation of tree crowns from aerial point clouds or stems from terrestrial point clouds (Kwak et al., 2007), leading to estimation error with the object-based CIs. Hence, methodological improvements in this area would benefit the detailed characterization of individual trees in general and the competitive stress in particular.

It is shown in this study that by using close-range terrestrial and low-altitude aerial point clouds, the competitive stress of trees can be quantified by characterizing its surroundings: the distance and the size of the neighboring trees considered as competitors (i.e., the object-based approach) or the magnitude of vegetation occupying the growing space around the tree (i.e., the point cloud-based approach). According to the assessments carried out in this study, accurate CI estimates were obtained in simple forest structures where the applied point clouds can characterize all the competing neighbor trees and their vegetative structures causing competition for resources. The findings of this study can improve forest management by providing tools to monitor the competitive stress of trees and how it evolves over time, which is needed for determining the timing of thinning or final cutting. It should be noted that such point cloud data that was used in this study to characterize competition can also be used to characterize increments in the stem dimensions and crown architecture if bitemporal data is available (Luoma et al., 2021; Sheppard et al., 2017; Yrttimaa et al., 2022). Having tools to measure the characteristics of the competitive environment and how it changes over time would be valuable input data for growth modeling (Weiskittel et al., 2011). With increased knowledge of how the dynamics of surrounding vegetation affect the allocation of

growth into different parts of the tree, it may be possible to develop silviculture further and to control the quality of harvested wood more precisely.

5. Conclusion

Studying competitive stress affecting individual trees is beneficial for understanding the process of tree growth which ultimately determines its architectural characteristics as well as wood properties. Therefore, assessing the magnitude of competition targeted at tree individuals is of interest for forest inventories and management planning. However, competition assessments based on *in situ* measurements are usually limited in terms of the spatiotemporal coverage and the level of detail incorporated in such observations, including the location and tree dimensions. Laser scanning technologies such as TLS and low-altitude ALS can accurately characterize the 3D structure of individual trees and forest stands, providing complimentary viewpoints for tree characterization. Hence, we assessed the capability of TLS and low-altitude ALS characterizing the competitive stress affecting individual trees in boreal forests using the object-based CIs to quantify the competitive status of a tree concerning its neighbor trees as well as the point cloud-based CIs to quantify the competitive status of a tree concerning the free space available on its surroundings. Comparison of these laser scanning-based CIs with the *in situ*-based CIs confirmed their potential but revealed some challenges related to accurate CI estimation using the point clouds. Point cloud occlusion and subsequent non-detection of all relevant neighboring trees – either tree individuals or vegetative structures – were the main obstacles in achieving accurate estimates for competition between trees. Overall, the competition effects described using low-altitude ALS and TLS data were very similar. This result suggests that although TLS can describe tree and canopy structures in much greater detail, low-altitude ALS data can provide similar results in describing competition. However, it is important to note that we used very detailed ALS data obtained from the flying altitude of 75 m, which is not available over large areas. Nonetheless, similar competition-describing metrics can be derived from sparser ALS data with a point density of 5 or more points per square meter. This kind of ALS dataset is widely available and mainly collected to support forest management and timber procurement. Thus, we presume that when forest resource data is collected using traditional ALS (i.e. flying altitudes hundreds or thousands of meters), tree competition could also be described using object-based methods. This could enable, for example, the timing of thinning operations and help prioritize the urgency of forest management activities.

CRediT authorship contribution statement

Ghasem Ronoud: Writing – original draft, Visualization, Methodology, Investigation, Conceptualization. **Maryam Poorazimy:** Writing – review & editing, Methodology, Conceptualization. **Tuomas Yrttimaa:** Writing – review & editing, Methodology. **Antero Kukko:** Resources, Funding acquisition. **Juha Hyyppä:** Resources, Funding acquisition. **Ninni Saarinen:** Writing – review & editing, Supervision, Methodology, Conceptualization. **Ville Kankare:** Writing – review & editing, Supervision, Methodology, Conceptualization. **Mikko Vastaranta:** Writing – review & editing, Supervision, Resources, Funding acquisition, Conceptualization.

Declaration of Competing Interest

The authors declare that they have no known competing financial interests or personal relationships that could have appeared to influence the work reported in this paper.

Data Availability

Data will be made available on request.

Acknowledgments

This research was funded by the Research Council of Finland (grant numbers 337127, 337655, 337656 315079, 345166, and 331711).

References

Axelsson, C.R., Lindberg, E., Persson, H.J., Holmgren, J., 2023. The use of dual-wavelength airborne laser scanning for estimating tree species composition and species-specific stem volumes in a boreal forest. Int. J. Appl. Earth Obs. Geoinf. 118, 103251. https://doi.org/10.1016/j.jag.2023.103251.

Bazezew, M.N., Hussin, Y.A., Kloosterman, E.H., 2018. Integrating airborne LiDAR and terrestrial laser scanner forest parameters for accurate above-ground biomass/carbon estimation in ayer hitam tropical forest, Malaysia. Int. J. Appl. Earth Obs. Geoinf. 73, 638–652. https://doi.org/10.1016/j.jag.2018.07.026.

Béland, M., Baldocchi, D.D., Widlowski, J.-L., Fournier, R.A., Verstraete, M.M., 2014. On seeing the wood from the leaves and the role of voxel size in determining leaf area distribution of forests with terrestrial LiDAR. Agric. For. Meteorol. 184, 82–97. https://doi.org/10.1016/j.agrformet.2013.09.005.

Béland, M., Widlowski, J.-L., Fournier, R.A., Côté, J.-F., Verstraete, M.M., 2011. Estimating leaf area distribution in savanna trees from terrestrial LiDAR measurements. Agric. For. Meteorol. 151, 1252–1266. https://doi.org/10.1016/j.agrformet.2011.05.004.

Bollandsås, O.M., Næsset, E., 2009. Weibull models for single-tree increment of Norway spruce, Scots pine, birch and other broadleaves in Norway. Scand. J. For. Res. 24, 54–66. https://doi.org/10.1080/02827580802477875.

Burkhart, H.E., Tomé, M., 2012. Modeling forest trees and stands. Model. For. Trees Stands 9789048131, 1–457. https://doi.org/10.1007/978-90-481-3170-9.

Calders, K., Adams, J., Armston, J., Bartholomeus, H., Bauwens, S., Bentley, L.P., Chave, J., Danson, F.M., Demol, M., Disney, M., Gaulton, R., Krishna Moorthy, S.M., Levick, S.R., Saarinen, N., Schaaf, C., Stovall, A., Terryn, L., Wilkes, P., Verbeeck, H., 2020. Terrestrial laser scanning in forest ecology: expanding the horizon. Remote Sens. Environ. 251, 112102. https://doi.org/10.1016/j.rse.2020.112102.

Casas, Á., García, M., Siegel, R.B., Koltunov, A., Ramírez, C., Ustin, S., 2016. Burned forest characterization at single-tree level with airborne laser scanning for assessing wildlife habitat. Remote Sens. Environ. 175, 231–241. https://doi.org/10.1016/j.rse.2015.12.044.

Contreras, M.A., Affleck, D., Chung, W., 2011. Evaluating tree competition indices as predictors of basal area increment in western Montana forests. For. Ecol. Manag. 262, 1939–1949. https://doi.org/10.1016/j.foreco.2011.08.031.

Dai, W., Yang, B., Liang, X., Dong, Z., Huang, R., Wang, Y., Li, W., 2019. Automated fusion of forest airborne and terrestrial point clouds through canopy density analysis. ISPRS J. Photogramm. Remote Sens. 156, 94–107. https://doi.org/10.1016/j.isprsjprs.2019.08.008.

Eid, T., Tuhus, E., 2001. Models for individual tree mortality in Norway. For. Ecol. Manag. 154, 69–84. https://doi.org/10.1016/S0378-1127(00)00634-4.

Fassnacht, F.E., White, J.C., Wulder, M.A., Næsset, E., 2024. Remote sensing in forestry: current challenges, considerations and directions. For. Int. J. For. Res. 97, 11–37. https://doi.org/10.1093/forestry/cpad024.

Fichtner, A., Härdtle, W., 2021. Forest Ecosystems: A Functional and Biodiversity Perspective 383–405. https://doi.org/10.1007/978-3-030-57710-0_16.

Giannetti, F., Puletti, N., Quatrini, V., Travaglini, D., Bottalico, F., Corona, P., Chirici, G., 2018. Integrating terrestrial and airborne laser scanning for the assessment of single-tree attributes in Mediterranean forest stands. Eur. J. Remote Sens. 51, 795–807. https://doi.org/10.1080/22797254.2018.1482733.

Hegyi, F., 1974. A simulation model for managing jack-pine stands. Growth Model Tree Stand Simul. 74–90.

Hilker, T., Coops, N.C., Newnham, G.J., van Leeuwen, M., Wulder, M.A., Stewart, J., Culvenor, D.S., 2012. Comparison of terrestrial and airborne LiDAR in describing stand structure of a thinned lodgepole pine forest. J. For. 110, 97–104. https://doi.org/10.5849/jof.11-003.

Hilker, T., van Leeuwen, M., Coops, N.C., Wulder, M.A., Newnham, G.J., Jupp, D.L.B., Culvenor, D.S., 2010. Comparing canopy metrics derived from terrestrial and airborne laser scanning in a Douglas-fir dominated forest stand. Trees 24, 819–832. https://doi.org/10.1007/s00468-010-0452-7.

Hui, G., Wang, Y., Zhang, G., Zhao, Z., Bai, C., Liu, W., 2018. A novel approach for assessing the neighborhood competition in two different aged forests. For. Ecol. Manag. 422, 49–58. https://doi.org/10.1016/j.foreco.2018.03.045.

Hyyppä, J., Yu, X., Hyyppä, H., Vastaranta, M., Holopainen, M., Kukko, A., Kaartinen, H., Jaakkola, A., Vaaja, M., Koskinen, J., Alho, P., 2012. Advances in forest inventory using airborne laser scanning. Remote Sens 4, 1190–1207. https://doi.org/10.3390/rs4051190.

Isenburg, M., 2019. LAStools—Efficient LiDAR Processing Software,(version 181001 academic); rapidlasso GmbH: Gilching, Germany.

Kalliovirta, J., Tokola, T., 2005. Functions for estimating stem diameter and tree age using tree height, crown width and existing stand database information. Silva Fenn. 39, 227–248.

Khosravipour, A., Skidmore, A.K., Isenburg, M., 2016. Generating spike-free digital surface models using LiDAR raw point clouds: a new approach for forestry applications. Int. J. Appl. Earth Obs. Geoinf. 52, 104–114. https://doi.org/10.1016/j.jag.2016.06.005.

Kükenbrink, D., Schneider, F.D., Leiterer, R., Schaepman, M.E., Morsdorf, F., 2017. Quantification of hidden canopy volume of airborne laser scanning data using a

voxel traversal algorithm. Remote Sens. Environ. 194, 424–436. https://doi.org/10.1016/j.rse.2016.10.023.
Kwak, D.-A., Lee, W.-K., Lee, J.-H., Biging, G.S., Gong, P., 2007. Detection of individual trees and estimation of tree height using LiDAR data. J. For. Res. 12, 425–434. https://doi.org/10.1007/s10310-007-0041-9.
Lexerød, N., Eid, T., 2005. Recruitment models for Norway spruce, scots pine, birch and other broadleaves in young growth forests in Norway. Silva Fenn. 39, 391–406. https://doi.org/10.14214/sf.376.
Liang, X., Hyyppä, J., Kaartinen, H., Lehtomäki, M., Pyörälä, J., Pfeifer, N., Holopainen, M., Brolly, G., Francesco, P., Hackenberg, J., Huang, H., Jo, H.-W., Katoh, M., Liu, L., Mokroš, M., Morel, J., Olofsson, K., Poveda-Lopez, J., Trochta, J., Wang, D., Wang, J., Xi, Z., Yang, B., Zheng, G., Kankare, V., Luoma, V., Yu, X., Chen, L., Vastaranta, M., Saarinen, N., Wang, Y., 2018. International benchmarking of terrestrial laser scanning approaches for forest inventories. ISPRS J. Photogramm. Remote Sens. 144, 137–179. https://doi.org/10.1016/j.isprsjprs.2018.06.021.
Liang, X., Kankare, V., Hyyppä, J., Wang, Y., Kukko, A., Haggrén, H., Yu, X., Kaartinen, H., Jaakkola, A., Guan, F., Holopainen, M., Vastaranta, M., 2016. Terrestrial laser scanning in forest inventories. ISPRS J. Photogramm. Remote Sens. 115, 63–77. https://doi.org/10.1016/j.isprsjprs.2016.01.006.
Lin, C., Thomson, G., Popescu, S., 2016. An IPCC-compliant technique for forest carbon stock assessment using airborne LiDAR-derived tree metrics and competition index. Remote Sens 8, 528. https://doi.org/10.3390/rs8060528.
Lo, C.-S., Lin, C., 2013. Growth-competition-based stem diameter and volume modeling for tree-level forest inventory using airborne LiDAR data. IEEE Trans. Geosci. Remote Sens. 51, 2216–2226. https://doi.org/10.1109/TGRS.2012.2211023.
Luoma, V., Yrttimaa, T., Kankare, V., Saarinen, N., Pyörälä, J., Kukko, A., Kaartinen, H., Hyyppä, J., Holopainen, M., Vastaranta, M., 2021. Revealing changes in the stem form and volume allocation in diverse boreal forests using two-date terrestrial laser scanning. Forests 12, 835. https://doi.org/10.3390/f12070835.
Ma, Q., Su, Y., Tao, S., Guo, Q., 2018. Quantifying individual tree growth and tree competition using bi-temporal airborne laser scanning data: a case study in the Sierra Nevada Mountains, California. Int. J. Digit. Earth 11, 485–503. https://doi.org/10.1080/17538947.2017.1336578.
Maas, H. -G., Bienert, A., Scheller, S., Keane, E., 2008. Automatic forest inventory parameter determination from terrestrial laser scanner data. Int. J. Remote Sens. 29, 1579–1593. https://doi.org/10.1080/01431160701736406.
Maltamo, M., Hyyppä, J., Malinen, J., 2006. A comparative study of the use of laser scanner data and field measurements in the prediction of crown height in boreal forests. Scand. J. For. Res. 21, 231–238. https://doi.org/10.1080/02827580600700353.
Maltamo, M., Mustonen, K., Hyyppä, J., Pitkänen, J., Yu, X., 2004. The accuracy of estimating individual tree variables with airborne laser scanning in a boreal nature reserve. Can. J. For. Res. 34, 1791–1801. https://doi.org/10.1139/x04-055.
Metz, J., Seidel, D., Schall, P., Scheffer, D., Schulze, E.-D., Ammer, C., 2013. Crown modeling by terrestrial laser scanning as an approach to assess the effect of aboveground intra- and interspecific competition on tree growth. For. Ecol. Manag. 310, 275–288. https://doi.org/10.1016/j.foreco.2013.08.014.
Meyer, F., Beucher, S., 1990. Morphological segmentation. J. Vis. Commun. Image Represent. 1, 21–46. https://doi.org/10.1016/1047-3203(90)90014-M.
Muhojoki, J., Tavi, D., Hyyppä, E., Lehtomäki, M., Faitli, T., Kaartinen, H., Kukko, A., Hakala, T., Hyyppä, J., 2024. Benchmarking under- and above-canopy laser scanning solutions for deriving stem curve and volume in easy and difficult boreal forest conditions. Remote Sens 16, 1721. https://doi.org/10.3390/rs16101721.
Novotny, J., Navratilova, B., Albert, J., Cienciala, E., Fajmon, L., Brovkina, O., 2021. Comparison of spruce and beech tree attributes from field data, airborne and terrestrial laser scanning using manual and automatic methods. Remote Sens. Appl. Soc. Environ. 23, 100574. https://doi.org/10.1016/j.rsase.2021.100574.
Olivier, M.-D., Robert, S., Fournier, R.A., 2016. Response of sugar maple (Acer saccharum, Marsh.) tree crown structure to competition in pure versus mixed stands. For. Ecol. Manag. 374, 20–32. https://doi.org/10.1016/j.foreco.2016.04.047.
Pedersen, R.Ø., Bollandsås, O.M., Gobakken, T., Næsset, E., 2012. Deriving individual tree competition indices from airborne laser scanning. For. Ecol. Manag. 280, 150–165. https://doi.org/10.1016/j.foreco.2012.05.043.
Pedersen, R.Ø., Næsset, E., Gobakken, T., Bollandsås, O.M., 2013. On the evaluation of competition indices - the problem of overlapping samples. For. Ecol. Manag. 310, 120–133. https://doi.org/10.1016/j.foreco.2013.07.040.
Perry, D.A., 1985. the Competition Process in Forest Stands. Attrib. trees as Crop plants 481–506.
Persson, Å., Holmgren, J., Söderman, U., 2002. Detecting and measuring individual trees using an airborne laser scanner.
Pitkänen, T.P., Bianchi, S., Kangas, A., 2022. Quantifying the effects of competition on the dimensions of Scots pine and Norway spruce crowns. Int. J. Appl. Earth Obs. Geoinf. 112, 102941. https://doi.org/10.1016/j.jag.2022.102941.
Pont, D., Dungey, H.S., Suontama, M., Stovold, G.T., 2021. Spatial models with inter-tree competition from airborne laser scanning improve estimates of genetic variance. Front. Plant Sci. 11. https://doi.org/10.3389/fpls.2020.596315.
Poorazimy, M., Ronoud, G., Yu, X., Luoma, V., Hyyppä, J., Saarinen, N., Kankare, V., Vastaranta, M., 2022. Feasibility of Bi-temporal airborne laser scanning data in detecting species-specific individual tree crown growth of boreal forests. Remote Sens 14, 4845. https://doi.org/10.3390/rs14194845.
Raumonen, P., Kaasalainen, M., Markku, Å., Kaasalainen, S., Kaartinen, H., Vastaranta, M., Holopainen, M., Disney, M., Lewis, P., 2013. Fast automatic precision tree models from terrestrial laser scanner data. Remote Sens. 5, 491–520. https://doi.org/10.3390/rs5020491.
Rivas, J.J.C., González, J.G.Á., Aguirre, O., Hernández, F.J., 2005. The effect of competition on individual tree basal area growth in mature stands of Pinus cooperi Blanco in Durango (Mexico). Eur. J. For. Res. 124, 133–142. https://doi.org/10.1007/s10342-005-0061-y.
Rocha, K.D., Silva, C.A., Cosenza, D.N., Mohan, M., Klauberg, C., Schlickmann, M.B., Xia, J., Leite, R.V., Almeida, D.R.A. de, Atkins, J.W., Cardil, A., Rowell, E., Parsons, R., Sánchez-López, N., Prichard, S.J., Hudak, A.T., 2023. Crown-level structure and fuel load characterization from airborne and terrestrial laser scanning in a longleaf pine (Pinus palustris Mill.) forest ecosystem. Remote Sens 15, 1002. https://doi.org/10.3390/rs15041002.
Ronoud, G., Poorazimy, M., Yrttimaa, T., Luoma, V., Huuskonen, S., Hynynen, J., Hyyppä, J., Saarinen, N., Kankare, V., Vastaranta, M., 2022. Terrestrial laser scanning in assessing the effect of different thinning treatments on the competition of scots pine (Pinus sylvestris L.) forests. Remote Sens 14, 5196. https://doi.org/10.3390/rs14205196.
Roussel, J.R., Auty, D., 2018. LidR: Airborne LiDAR data manipulation and visualization for forestry applications. R. CRAN Proj. 1, 1.
Seidel, D., Hoffmann, N., Ehbrecht, M., Juchheim, J., Ammer, C., 2015. How neighborhood affects tree diameter increment – New insights from terrestrial laser scanning and some methodical considerations. For. Ecol. Manag. 336, 119–128. https://doi.org/10.1016/j.foreco.2014.10.020.
Sheppard, J., Morhart, C., Hackenberg, J., Spiecker, H., 2017. Terrestrial laser scanning as a tool for assessing tree growth. iForest - Biogeosci. 10, 172–179. https://doi.org/10.3832/ifor2138-009.
Stephenson, N.L., Das, A.J., Condit, R., Russo, S.E., Baker, P.J., Beckman, N.G., Coomes, D.A., Lines, E.R., Morris, W.K., Rüger, N., Álvarez, E., Blundo, C., Bunyavejchewin, S., Chuyong, G., Davies, S.J., Duque, Á., Ewango, C.N., Flores, O., Franklin, J.F., Grau, H.R., Hao, Z., Harmon, M.E., Hubbell, S.P., Kenfack, D., Lin, Y., Makana, J.-R., Malizia, A., Malizia, L.R., Pabst, R.J., Pongpattananurak, N., Su, S.-H., Sun, I.-F., Tan, S., Thomas, D., van Mantgem, P.J., Wang, X., Wiser, S.K., Zavala, M. A., 2014. Rate of tree carbon accumulation increases continuously with tree size. Nature 507, 90–93. https://doi.org/10.1038/nature12914.
Su, Y., Guo, Q., Fry, D.L., Collins, B.M., Kelly, M., Flanagan, J.P., Battles, J.J., 2016. A Vegetation mapping strategy for conifer forests by combining airborne LiDAR data and aerial imagery. Can. J. Remote Sens. 42, 1–15. https://doi.org/10.1080/07038992.2016.1131114.
Szwagrzyk, J., Szewczyk, J., Maciejewski, Z., 2012. Shade-tolerant tree species from temperate forests differ in their competitive abilities: A case study from Roztocze, south-eastern Poland. For. Ecol. Manag. 282, 28–35. https://doi.org/10.1016/j.foreco.2012.06.031.
Tempel, D.J., Gutiérrez, R.J., Battles, J.J., Fry, D.L., Su, Y., Guo, Q., Reetz, M.J., Whitmore, S.A., Jones, G.M., Collins, B.M., Stephens, S.L., Kelly, M., Berigan, W.J., Peery, M.Z., 2015. Evaluating short- and long-term impacts of fuels treatments and simulated wildfire on an old-forest species. Ecosphere 6. https://doi.org/10.1890/ES15-00234.1.
Terryn, L., Calders, K., Bartholomeus, H., Bartolo, R.E., Brede, B., D'hont, B., Disney, M., Herold, M., Lau, A., Shenkin, A., Whiteside, T.G., Wilkes, P., Verbeeck, H., 2022. Quantifying tropical forest structure through terrestrial and UAV laser scanning fusion in Australian rainforests. Remote Sens. Environ. 271, 112912. https://doi.org/10.1016/j.rse.2022.112912.
Tomé, M., Burkhart, H.E., 1989. Distance-dependent competition measures for predicting growth of individual trees. For. Sci. 35, 816–831. https://doi.org/10.1093/forestscience/35.3.816.
Tompalski, P., Coops, N., White, J., Wulder, M., 2016. Enhancing forest growth and yield predictions with airborne laser scanning data: increasing spatial detail and optimizing yield curve selection through template matching. Forests 7, 255. https://doi.org/10.3390/f7110255.
Twery, M.J., Weiskittel, A.R., 2013. Forest-management modelling. In: Environmental Modelling. Wiley, pp. 379–398. https://doi.org/10.1002/9781118351475.ch23.
Vauhkonen, J., Ene, L., Gupta, S., Heinzel, J., Holmgren, J., Pitkanen, J., Solberg, S., Wang, Y., Weinacker, H., Hauglin, K.M., Lien, V., Packalen, P., Gobakken, T., Koch, B., Naesset, E., Tokola, T., Maltamo, M., 2012. Comparative testing of single-tree detection algorithms under different types of forest. Forestry 85, 27–40. https://doi.org/10.1093/forestry/cpr051.
Vauhkonen, J., Maltamo, M., McRoberts, R.E., Næsset, E., 2014. Introduction to Forestry Applications of Airborne Laser Scanning 1–16. https://doi.org/10.1007/978-94-017-8663-8_1.
Versace, Gianelle, Frizzera, Tognetti, Garfì, Dalponte, 2019. Prediction of competition indices in a norway spruce and silver fir-dominated forest using lidar data. Remote Sens 11, 2734. https://doi.org/10.3390/rs11232734.
Wang, Y., Hyyppa, J., Liang, X., Kaartinen, H., Yu, X., Lindberg, E., Holmgren, J., Qin, Y., Mallet, C., Ferraz, A., Torabzadeh, H., Morsdorf, F., Zhu, L., Liu, J., Alho, P., 2016. International benchmarking of the individual tree detection methods for modeling 3-D canopy structure for silviculture and forest ecology using airborne laser scanning. IEEE Trans. Geosci. Remote Sens. 54, 5011–5027. https://doi.org/10.1109/TGRS.2016.2543225.
Weiskittel, A.R., Hann, D.W., Kershaw, J.A., Vanclay, J.K., 2011. Forest Growth and Yield Modeling. For. Growth Yield Model. https://doi.org/10.1002/9781119998518.
Wensel, L.C., Meerschaert, W.J., Biging, G.S., 1987. Tree height and diameter growth models for Northern California conifers. Hilgardia 55, 1–20. https://doi.org/10.3733/hilg.v55n08p020.
White, J.C., Coops, N.C., Wulder, M.A., Vastaranta, M., Hilker, T., Tompalski, P., 2016. Remote sensing technologies for enhancing forest inventories: a review. Can. J. Remote Sens. 42, 619–641. https://doi.org/10.1080/07038992.2016.1207484.
Wulder, M.A., Franklin, S.E., 2003. Remote sensing of forest environments, introduction. the transition from theory to information. Remote Sens. For. Environ. 3–12.

Yrttimaa, T., Luoma, V., Saarinen, N., Kankare, V., Junttila, S., Holopainen, M., Hyyppä, J., Vastaranta, M., 2022. Exploring tree growth allometry using two-date terrestrial laser scanning. For. Ecol. Manag. 518. https://doi.org/10.1016/j.foreco.2022.120303.

Yrttimaa, T., Saarinen, N., Kankare, V., Liang, X., Hyyppä, J., Holopainen, M., Vastaranta, M., 2019. Investigating the feasibility of multi-scan terrestrial laser scanning to characterize tree communities in southern boreal forests. Remote Sens 11, 1423. https://doi.org/10.3390/rs11121423.

Yrttimaa, T., Saarinen, N., Kankare, V., Hynynen, J., Huuskonen, S., Holopainen, M., Hyyppä, J., Vastaranta, M., 2020. Performance of terrestrial laser scanning to characterize managed Scots pine (Pinus sylvestris L.) stands is dependent on forest structural variation. ISPRS J. Photogramm. Remote Sens. 168, 277–287. https://doi.org/10.1016/j.isprsjprs.2020.08.017.

Zhou, M., Lei, X., Lu, J., Gao, W., Zhang, H., 2022. Comparisons of competitor selection approaches for spatially explicit competition indices of natural spruce-fir-broadleaf mixed forests. Eur. J. For. Res. 141, 177–211. https://doi.org/10.1007/s10342-021-01430-8.